The Solar System Beyond The Planets

Audrey Delsanti and David Jewitt

Institute for Astronomy, University of Hawaii, 2680 Woodlawn Drive, Honolulu, HI 96822
delsanti@ifa.hawaii.edu, jewitt@ifa.hawaii.edu

Summary. The Kuiper belt contains a vast number of objects in a flattened, ring-like volume beyond the orbit of Neptune. These objects are collisionally processed relics from the accretion disk of the Sun and, as such, they can reveal much about early conditions in the Solar system. At the cryogenic temperatures prevailing beyond Neptune, volatile ices have been able to survive since the formation epoch 4.5 Gyr ago. The Kuiper belt is the source of the Centaurs and the Jupiter-family comets. It is also a local analogue of the dust disks present around some nearby main-sequence stars. While most Kuiper belt objects are small, roughly a dozen known examples have diameters of order 1000 km or more, including Pluto and the recently discovered (and possibly larger) giant Kuiper belt objects 2003 UB_{313}, 2003 EL_{61} (a binary and a triple system, resp.) and 2005 FY_9.

1 Introduction

As is well known, Pluto was discovered in 1930 as the result of a search motivated by Percival Lowell's prediction of a 9th planet. Lowell based his prediction on anomalies in the motion of Uranus that could not be explained by the gravitational tug of Neptune. In hindsight, we now know that these anomalies were simply astrometric errors, and that Lowell's prediction of Pluto was baseless. Nevertheless, Clyde Tombaugh found Pluto and he and many others assumed that it was the massive object predicted by Lowell (Tombaugh, 1961). Doubts about the correctness of this assumption were raised almost immediately, with the realization that the likely mass of Pluto was too small to measurably perturb Uranus or Neptune. Still, the planetary label stuck.

Pluto's true significance became apparent only in 1992, with the discovery of the trans-Neptunian object 1992 QB_1 (Jewitt & Luu, 1993). Since then, about 1000 Kuiper belt objects (KBOs) have been found, with sizes from a few 10's km to several 1000 km and orbits in a number of dynamically distinct classes. Their defining feature is that their semi-major axes are larger than that of Neptune (30 AU). Most have perihelia beyond 30 AU: the region inside Neptune's orbit tends to be dynamically unstable owing to strong perturbations from the giant planets. The known dynamical sub-types (their average orbital parameters are listed in Table 1) in the Kuiper Belt are:

Resonant Objects

The resonant objects are those trapped in mean-motion resonance with Neptune. The prime example is Pluto, which sits with a great many other KBOs in the 3:2 mean motion resonance at 39.5 AU. Occupancy in a mean-motion resonance conveys dynamical stability, by limiting the possibilities for close encounters between the trapped KBO and Neptune. Pluto, for example, has a perihelion distance ($q = 29.7$ AU) inside Neptune's orbit, but never encounters Neptune because the resonance ensures that the longitude of perihelion is separated from that of the planet by about $\pm 90^\circ$. The 3:2 resonance is the most densely populated and, to draw a parallel with the largest trapped object, the residents of this resonance are known as "Plutinos". Numerous other resonances are also occupied, including so-called secular resonances in which there is commensurability between the rates of precession of angular variables describing the orbits of the KBOs and corresponding quantities of the orbit of Neptune.

Classical Kuiper belt

The Classical Kuiper belt is effectively the region between the 3:2 mean motion resonance at 39.5 AU and the 2:1 mean motion resonance at 48 AU, excluding objects which are in those resonances. The first-detected objects in this region, like the prototype 1992 QB_1, have small inclinations, reminiscent of dynamical expectations that the Belt would be a dynamically cold (thin) structure left over from the accretion epoch. Later discoveries, however, have included a large number of highly inclined KBOs in the Classical region, and we now recognize that there are two populations superimposed in this region. The low inclination ("cold") population has $i \leq 4^\circ$ while the high inclination ("hot") population extends to inclinations of 30° to 40°, and possibly higher. As discussed below, there is some evidence for a difference between the physical properties of the hot and cold populations.

Scattered Objects

These are objects with perihelia in the $\sim$35 to 40 AU range and characteristically large eccentricities and inclinations. The first example found, 1996 TL_{66}, is typical with $a = 82.9$ AU, $e = 0.577$ and $i = 24^\circ$. The scattered objects, often called scattered disk objects (although their large inclinations more resemble a torus than a disk) are thought to have been lofted into eccentric orbits by weak scattering from Neptune (Morbidelli et al., 2004). In this scenario they would be survivors of a once much larger population that has been steadily depleted by Neptune perturbations over Solar system time. Recent work has shown that many scattered objects are in fact trapped in high order mean motion resonances, blurring at least the nomenclature and their distinction from the resonant population. The likely mechanism of emplacement of the bodies remains scattering by Neptune, however, so that the label is not entirely without meaning.

Detached Objects

Two objects, 2000 CR_{105} (Gladman et al., 2002) and (90377) Sedna (Brown et al., 2004), have perihelia so large that they cannot have been emplaced by gravitational interactions with Neptune, at least not in the same way as were the other scattered objects. These bodies define the class of detached objects (Emel'yanenko et al., 2003) also called "extended scattered disk" objects. Their emplacement might have been due to perturbations associated with a passing star (Morbidelli & Levison, 2004).

Table 1. Mean orbital elements of KBOs sub-classes and Centaurs

	a[AU]	$\bar{e}$	$\bar{i}$ [deg]	$N_{objects}$
Classical	39.4 < a <47.8	0.06	6.97	681
3:2 resonance	39.4	0.22	9.93	47
5:3 resonance	42.4	0.20	9.35	4
7:4 resonance	43.6	0.20	3.97	4
2:1 resonance	47.6	0.31	11.5	7
5:2 resonance	55.8	0.41	8.03	6
Scattered	>30	0.29	12.6	384
Centaurs	<35	0.31	12.9	57

2 Pluto and Other Large Kuiper belt Objects

About a dozen KBOs are now known with diameters in the 1000 km range and larger (Table 2). In July 2005, three Pluto-sized bodies were announced: 2003 UB_{313}, 2003 EL_{61} (both are binary systems) and 2005 FY_9. They are the result of an on-going survey dedicated to the search of bright KBOs (Trujillo & Brown, 2003). Indeed, results from previous surveys are in agreement to predict the existence of a few tens of KBOs of the size of Pluto, some of them possibly larger. Their discovery implies a large sky coverage (often limited to the ecliptic region and the Solar system invariable plane, where the high-inclination objects like 2003 UB_{313} spend only a small fraction of their orbit and are therefore more difficult to discover), a task that is time consuming. The Pan-STARRS project, a set of four 1.8m telescopes on top of Mauna Kea that will scan the whole available sky down to V$\sim$24 every couple of days, should significantly contribute to the discovery of new, large KBOs. In this section, we briefly describe the four largest objects known as October 2005.

Pluto

Observations of the orbital motion of Pluto and its main satellite Charon have given the combined mass of the pair as 1.5×10^{22} kg. This is only $\sim$0.2% of the mass of the Earth and five times less even than the mass of the Moon. "Mutual events", a series of occultations and eclipses visible as Earth passed through the orbital plane of Charon, have revealed many details of Pluto and Charon (see Table 3: Pluto) including the density, about 2000 kg m^{-3}, which suggests a composition about 70% rock by mass. The large specific angular momentum of the Pluto-Charon pair suggests that Charon may have formed by a glancing impact, presumably early in the history of the Solar system (Canup, 2005).

Independently of the mutual events, occultations of field stars by Pluto have revealed astounding details of this distant world. An atmosphere is present, with a pressure at 1250 km radius near 1 μbar (1 bar = 10^5 N m^{-2}, see Elliot et al., 1989). The occultation lightcurves show a steep drop in intensity near Pluto that cannot be accurately matched by a model of an isothermal atmosphere in hydrostatic equilibrium, leading to some ambiguity in the structure of the atmosphere and even the occultation radius of Pluto. The steep drop in the intensity can be explained by invoking a near-surface haze, or by invoking steep near-surface temperature gradients that would

Table 2. Large KBOs

Name	Type[a]	H^b	p[c]	D [km][d]	a [AU]	e	i[deg]	Multiple?
2003 UB_{313}	Scat	−1.2	0.6?	2600?	67.6	0.44	44.2	Yes
Pluto	3:2	−1.0	0.6	2320	39.5	0.25	17.1	Yes
2005 FY_9	Scat	0.3	0.6?	1250?	45.7	0.15	29.0	
2003 EL_{61}	Cla	0.4	0.6?	1200?	43.3	0.19	28.2	Yes
(90377) Sedna	Det	1.6	0.2?	<1500?	495	0.85	11.9	
(90482) Orcus	3:2	2.2	0.12?	∼1500	39.4	0.22	20.6	
(50000) Quaoar	Clas	2.6	0.12	1200∓200	43.5	0.03	8.0	
(28978) Ixion	3:2	3.2	0.09	1065∓165	39.6	0.24	19.6	
(55565) 2002 AW_{197}	Clas	3.2	0.1	890∓120	47.4	0.13	24.4	
(20000) Varuna	Clas	3.7	0.07±0.02	900∓140	43.0	0.05	17.2	

a: Dynamical type: 3:2 = resonant, Clas = Classical, Cen = Centaur, Scat = Scattered, Det = Detached
b: absolute magnitude
c: Geometric Albedo
d: Diameter

refract light from the occulted star away from the direction to the observer. In either case, the key uncertainty is the distance between the 1250 km reference radius probed by occultations and the surface, and this distance remains unknown. If we assume that the radius derived from mutual events is accurate, then the surface pressure (extrapolated from 1250 km) in the atmosphere must be near 30 μbar, but this value is uncertain by at least a factor of several. Pressures of this magnitude correspond to the vapor pressure above solid N_2 at Pluto's surface temperature ∼38 K. Recent observations of occultations of a bright star (Sicardy et al., 2003; Elliot et al., 2003) showed that the pressure at a given height is time-variable: the measured pressures were two times higher than in 1988, despite the greater heliocentric distance of Pluto. Presumably, time variations reflect seasonal variations in the insolation of patches of volatile matter exposed on the surface of Pluto.

Reflectance spectroscopy of Pluto reveals a variegated surface dominated by methane ice (CH_4) incorporated in frozen nitrogen (N_2). Carbon monoxide (CO) and some water ice (H_2O) are also detected. Hubble Space Telescope images evidenced some dark and bright areas over the surface. Bright areas are most probably covered by nitrogen and water ice, whereas the origin of dark areas is less clear. Methane is believed to be destroyed over time under the effect of the steady flux of ions and UV radiations (from solar wind and cosmic rays) that hits the surface. Laboratory work shows that such processes lead to the formation of dark-colored, complex organic compounds. The abundance of methane on the surface therefore indicates that a replenishment mechanism should be acting. At Pluto's surface equilibrium temperature (∼40K), methane can be volatile and mix with more volatile nitrogen to form a tenuous, weakly bound atmosphere. With seasonal variations of pressure, one can expect a future redeposition of frozen methane and nitrogen over the surface. A subsurface methane source is also invoked, that would replenish the surface through cryovolcanism, as hypothesized for

Neptune's satellite: Triton.

Two faint satellites (visible magnitude ∼23 and 23.4) were discovered in May 2005 on Hubble Space Telescope images (Weaver et al., 2005). They both are on a near circular orbit far outside Charon's. Preliminary studies give distances to the Pluto system barycenter of 64,700km and 49,500km for the brightest and the faintest satellite resp., corresponding to orbital periods of ∼38 and ∼25 days. All three satellites (including Charon) are orbiting on approximately the same plane. The project that lead to this discovery was aimed at mapping Pluto's sphere of gravitational influence: no other detection was claimed down to a magnitude of V∼27, which means that if any other satellite exists, it should be smaller than 20km in diameter. From the apparent brightness of the discovered satellites, the approximate diameters are estimated in the range 40km–180km.

Pluto is now known as a quadruple system. We can expect that several other multiple systems will be discovered in the Kuiper belt in the near future (the first triple system, 2003 EL_{61} was announced in December 2005). Further studies of these two new satellites will lead to improved estimates of the mass and density of Pluto and Charon and bring constraints on the formation scenario and tidal evolution of the whole system (and on the other KBO multiple systems).

Table 3. Parameters of the Pluto system

Object	Mass [kg]	Radius [km]	Density[g/cm^3]	a [km][a]	P [days][b]
Pluto	1.32×10^{22}	1160	2.0	—	6.37
Charon	1.6×10^{21}	625	1.7	19,400	6.37
S/2005 P 1	—	25-80?	—	64,700?	38.2?
S/2005 P 2	—	20-70?	—	49,500?	25.5?

a: semi-major axis of the orbit around the barycenter of the Pluto system
b: rotation period (Pluto), orbital period (Charon, S/2005 P 1, S/2005 P 2)

2003 UB_{313}

2003 UB_{313} is a scattered-disk object with an extremely high orbital inclination (44^o). It is currently located near aphelion at 97 AU from the Sun. With a semi-major axis of ∼68 AU, it will reach perihelion at 38 AU in ∼250 years: its surface will probably undergo significant seasonal changes on the way. Its albedo is not determined yet, but even with the most constraining assumptions, 2003 UB_{313} is likely to be larger than Pluto. Preliminary spectroscopic studies (Brown et al., 2005a) show that it has a methane dominated surface, very close to that of Pluto. The optical spectral slope, however, is less red. This is the first time methane has been firmly detected on a KBO other than on Pluto. Unlike the methane bands on Pluto, those on 2003 UB_{313} show no shift in wavelength that might be attributed to solution in solid nitrogen. Equilibrium surface temperatures are expected to be ∼30K at 97 AU. The corresponding vapor pressure over pure methane ice makes it in-volatile: it is most likely present on the surface as an ice, segregated from other components. However, as 2003 UB_{313} approaches

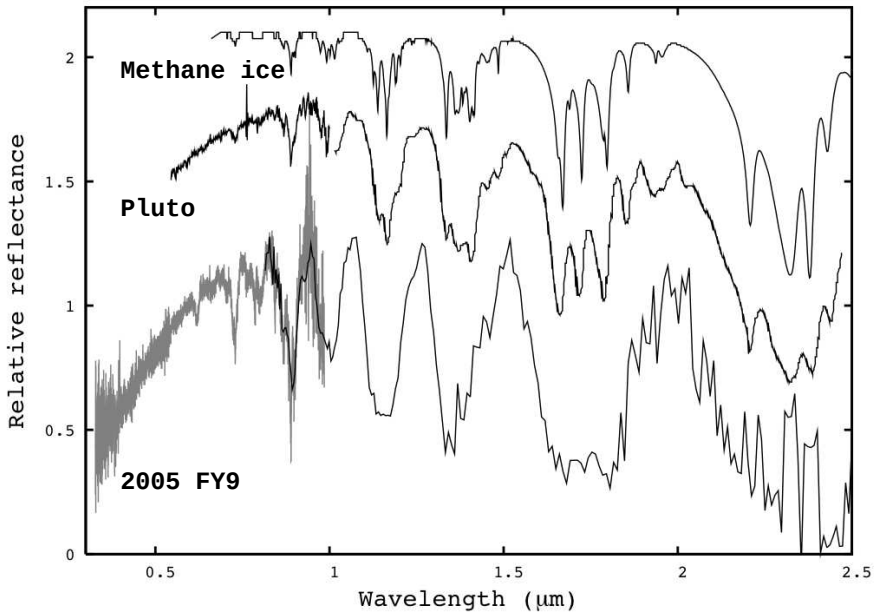

Fig. 1. Reflectance spectra of laboratory methane ice, Pluto (Grundy & Fink, 1996), and 2005 FY_9. Spectra are normalized at 0.6μm and vertically shifted for clarity. Pluto and 2005 FY_9 show very similar chemical surface composition. Figure from Licandro et al. (2006).

the Sun, methane will become volatile again and might mix with (not detected yet) nitrogen in a tenuous atmosphere, as for Pluto. 2003 UB_{313} therefore provides a low-temperature analog to study processes occurring on Pluto's surface. One possibility is that the presence of methane might be a characteristic of the largest KBOs, the smaller bodies being too small to retain it on their surface due to higher escape rates, or being unable to produce it owing to their frigid interiors.

A faint satellite has been reported around 2003 UB_{313} (with a fractional brightness of 2% of the primary). This satellite is much fainter than other KBO satellites and may have a different origin. The preliminary binary system characteristics favor the impact formation scenario (see Section 3).

2005 FY_9

2005 FY_9 is the third brightest known KBO (in absolute magnitude, after 2003 UB_{313} and Pluto). Its size may approach that of Pluto. With a semi-major axis of 46 AU, a perihelion of 39 AU and an inclination of $\sim 29^o$, it belongs to the classical KBOs family. Preliminary spectroscopic studies (Licandro et al., 2006) reveal the presence of methane (as in Pluto and 2003 UB_{313}). The methane lines detected are very close to those of laboratory pure methane ice. So far, no other ices such as N_2 or water ice were detected. The visible data show a spectroscopically red surface (similar to Pluto) which is compatible with the presence of complex organic compounds. Its general similarities

with Pluto (size, surface composition, heliocentric range) make 2005 FY_9 a good candidate to hold a tenuous, bound atmosphere. This hypothesis can be observationally tested in the future during an occultation of a star by 2005 FY_9. According to Brown et al. (2005b), no satellite was discovered within 0.4 arc-seconds of 2005 FY_9 and with a brightness of more than 0.5% of the object. This KBO will be the object of extensive studies.

2003 EL_{61}

2003 EL_{61} is the fourth brightest known KBO, and its size should be about that of Pluto. Early studies revealed both water ice on its surface and the presence of two satellites. The first satellite is on a near circular orbit at 49,500km from 2003 EL_{61}. Preliminary results (Brown et al., 2005c) show that the orbital period of the system is ∼49 days and the satellite brightness is 6% of 2003 EL_{61} (for reference, Pluto-Charon has an orbital period of 6.4 days and a flux ratio of 20). The mass of this system is estimated to 4×10^{21}kg which is 32% the mass of Pluto. The rotation of 2003 EL_{61} (∼4h, Rabinowitz et al., 2005, to be confirmed by further studies), is extremely fast. From the mass of the system and the rapid rotation period of the primary (which should lead to extreme rotational deformations), first estimations give a length of the primary of 1900 to 2500km, a mean density of 2600 to 3300 kg m^{-3} (consistent with Pluto) and a visual albedo greater than 60%. The parameters of this system are in partial agreement with an impact formation scenario (see Sec. 3) as for Pluto. In that case, tidal evolution will modify the eccentricity and orbital period of the system over time, with an amplitude determined by the strengthness of both the primary and the satellite. Another possibility is that this pair formed by capture (see Sec. 3), and the semi-major axis subsequently shrunk to the current one owing to dynamical friction. The current parameters of the system only partially match this scenario. As these lines are written, a second satellite is detected. Its brightness is 1.5% that of 2003 EL_{61}. Preliminary circular orbit fits (Brown et al., 2005b) give a semi-major axis of 39,300 km and an orbital period of 34 days. Its orbital plane is inclined of ∼40 degrees with respect to the other satellite's plane. The presence of multiple satellites around giant KBOs (as for Pluto) might point towards a formation in a disk, although this possibility requires further exploration.

Unfortunately, mutual events are not predicted in the near future and the characterization of 2003 EL_{61} (as regards mass, density, etc) will consequently be much poorer than for Pluto.

3 Binaries and multiple systems

Pluto's main satellite, Charon, was discovered as late as 1979 in photographic images taken to refine the orbit of this "planet" about the Sun. Pluto-Charon became the first-recognized of many Kuiper belt binaries (see Table 3). In fact, the Pluto-Charon system is synchronously locked, with the primary and secondary having the same spin period as the orbital period about the barycenter. This is a natural state for a binary in which gravitational tides are strong. Tides on the primary raised by the secondary (and vice-versa) raise a bulge on which gravitational torques act to bring the orbital and spin periods to the same value. With the Pluto-Charon separation of ∼20,000 km, the tidal dissipation time is small compared to the age of the Solar system, and a

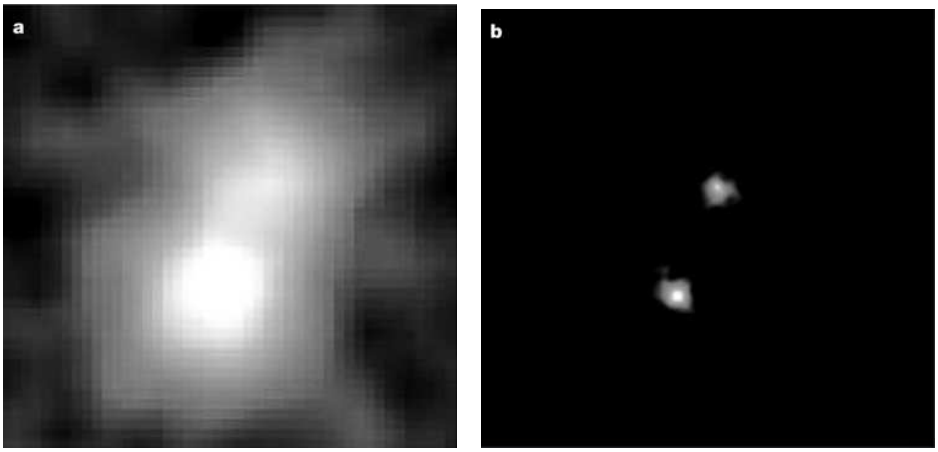

Fig. 2. The first discovered binary after Pluto-Charon, 1998 WW_{31}, as seen from the ground at CFHT on 2001 September 12 (left) and from the Hubble Space Telescope on September 9, 2001 (right). Separation is 0.59 arcsec on both images (same scale), semi-major axis of the system is ∼20,000 km. Images from Veillet et al. (2002).

Table 4. Parameters of the multiple KBOs

Object	a [km][a]	e[b]	i[deg][c]	Type[d]	Q[arc-sec][e]	P[days][f]	Δmag
Pluto				3:2			
Charon	19,400	0.00	96	—	0.9	6.4	3.2
S/2005 P1	64,700?	—	—	—	2.2	38.3?	9.0
S/2005 P2	49,400?	—	—	—	1.7	25.5?	9.4
1998 WW_{31}	22,300	0.8	42	Cla	1.2	574	0.4
(88611) 2001 QT_{297}	—	—	—	Cla	0.6	—	0.5
2001 QW_{322}	—	—	—	Cla	4.0	—	0.4
1999 TC_{36}	—	—	—	3:2	0.4	—	1.9
(26308) 1998 SM_{165}	—	—	—	2:1	0.2	—	1.9
(58534) 1997 CQ_{29}	—	—	—	Cla	0.2	—	0.3
2000 CF_{105}	—	—	—	Cla	0.8	—	0.9
2001 QC_{298}	—	—	—	Cla	0.17	—	N/A
2003 EL_{61}				Scat			
S/2005 (2003 EL_{61}) 1	49,500±400	0.050±0.003	234.8±0.3	—	1.3	49.12±0.03	3.3
S/2005 (2003 EL_{61}) 2	39,300?	—	—	—	1.0	34.1?	4.5
2003 UB_{313}	36,000	—	—	Scat	0.5	14	4.2

a: semi-major axis of the binary system
b: eccentricity
c: inclination
d: Dynamical type: 3:2, 2:1 = resonant, Clas = Classical, Scat = Scattered
e: Angular separation
f: Orbital period

synchronously locked system is the result.

The mechanisms by which the Kuiper belt binaries formed remain unidentified. Close binaries in nearly circular orbits, like Pluto-Charon and 2003 UB_{313}, suggest a collisional origin in which the satellite was blasted out of the primary by an ancient impact. Numerical simulations have shown that glancing impacts can produce bound satellites, at least over a range of carefully selected initial conditions (Canup 2005).

The wide, eccentric binaries that are seen elsewhere in the Kuiper belt must have a different origin, and several have already been suggested. In an early, dense Kuiper belt consisting of objects having a wide range of sizes, the process called "dynamical friction" might have acted to stabilize objects in wide binaries. In this process, the collective effects of the smaller objects exert a net force on massive bodies passing through them. One prediction of this model is that the fraction of binaries should increase as the separation decreases (Goldreich et al 2002). It is also possible that a dense early Kuiper belt could have a significant number of three-body interactions. In these, scattering between bodies can result in the ejection of one, which carries excess energy from the system and leaves behind a stable binary (Weidenschilling 2002). Three-body captures result mainly in wide binaries, and the detection of a substantial fraction of close binaries would require another explanation. From lightcurve studies, the fraction of contact binaries (perhaps products of continued dynamical friction) has been estimated as 10% to 20% (Sheppard & Jewitt, 2004).

The common feature of the binary formation models is that they all assume an initial dense phase, with densities $\sim$100 to $\sim$1000 times the present value in the trans-Neptunian region. If these conditions once prevailed, it is reasonable to assume that binaries were both formed and dissociated in an active early epoch, probably in association with or soon after formation. The existing suite of binaries are merely the survivors from this long-gone stage.

4 Observed Structure of the Kuiper belt

4.1 Inclination distribution and Velocity dispersion

Early models of the Kuiper belt predicted a modest range of inclinations of $\sim 1^\circ$ due to gravitational stirring by Neptune (e.g. Holman & Wisdom, 1993). The observed belt is much thicker, as may be seen in Figure 3 which shows an unbiased inclination distribution. The thickness of the Kuiper belt is directly related to the velocity dispersion amongst the objects within it. Careful measurements show that the velocity dispersion is now about 1.6 km s^{-1} (Trujillo et al., 2001). At this speed, KBOs shatter and pulverize each other when they collide instead of sticking and growing. The implication is that the velocity dispersion has been pumped up by some process (or processes) since the epoch of formation, when the velocity dispersion would have been an order of magnitude or more smaller than now. What could have done this? It is known that resonance trapping tends to pump up the inclinations of the objects that become trapped (Malhotra, 1995). This resonance pumping can explain why Pluto has $i \sim 17^\circ$, for example, but it is only a partial answer for the belt as whole because the resonant objects are a minority population. For the scattered disk objects, it is likely that the inclinations were amplified by the same scattering events that launched KBOs onto

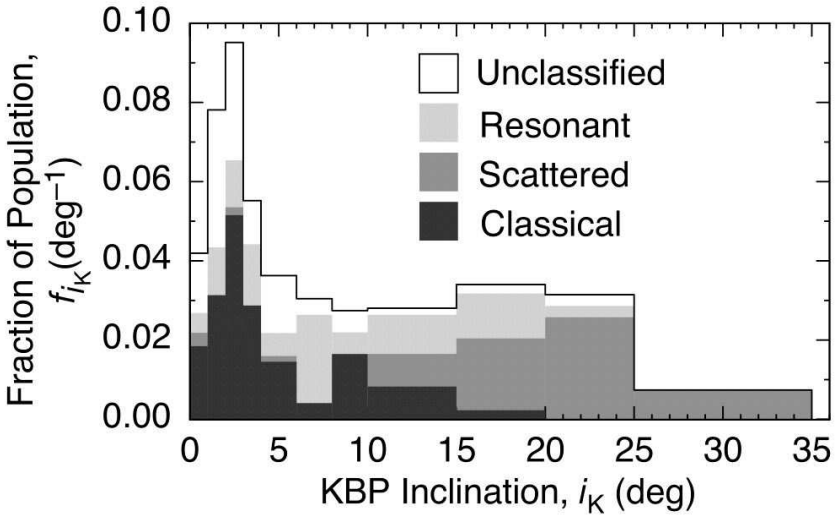

Fig. 3. Distributions of the inclinations of Kuiper belt objects in the resonant, scattered and classical populations (dynamically unclassified objects are also shown). The classical objects are bimodally distributed, with the cold and hot populations having peaks near 3° and 8°. The resonant and scattered populations show broad inclination distributions extending to 20° and above. Figure from Elliot et al. (2005).

their highly eccentric orbits: numerical simulations of this Neptune scattering produce inclination distributions broadly similar to the one observed (Gomes, 2003b).

More problematic is the inclination distribution of the classical objects which, as shown in Figure 3, is bimodal. This suggests that the classical belt has a composite structure. The cold (with red surfaces, as described in Section 5.1) classical KBOs maybe objects originally formed beyond Neptune and swept out by resonances during Neptune's migration phase. The hot (with neutral to red surfaces) classical KBOs may have been scattered outwards by the inner giant planets during the planetary migration phase and captured in orbits external to Neptune's (Gomes, 2003a). Why the cold and hot classical KBOs should have different color patterns is unknown and unspecified in this model, but the idea that the differences in the inclination and color distributions is somehow related to a difference in formation locations is attractive.

Still other causes of the broad inclination distribution have been suggested. It is possible that a star, passing ∼150 to 250 AU from the Sun, is responsible for observed structures in the Kuiper belt, notably the "edge" to the classical belt at about 47 AU to 48 AU (Ida et al., 2000). Perturbations from this star could stir up the belt, exciting the precursor disk into the puffy distribution we see now (and maybe truncating further growth of the KBOs in the process). The likelihood of a sufficiently close (∼150 AU) stellar encounter in the modern epoch is negligible: such interactions might have been common if the Sun were born in a dense cluster of stars.

4.2 Radial extent

The classical belt has an edge near the 2:1 mean motion resonance (47 AU to 48 AU) in the sense that the distribution of semi-major axes is truncated at about this radial distance (Jewitt et al., 1998; Allen et al., 2001; Trujillo et al., 2001). It is not known if this is a real edge, or just the inner boundary of a gap, with the surface density of objects increasing to a high value at some larger radius. Orbits of the scattered disk objects extend over a much larger range of distances. The most extreme objects reach aphelia near 1000 AU (the current record is 2000 OO_{67}, which reaches 1014 AU) and others yet to be found must push further out towards the inner Oort Cloud. It is probably misleading to think of a distinct boundary to the Kuiper belt, or a sharp junction between it and the Oort cloud. Dynamical models tend to suggest that the past histories of the Belt and the Cloud are intertwined, so that no absolute distinction is possible.

4.3 Mass and Size Distribution

Optical surveys give the number of objects as a function of apparent brightness. The precise conversion to size distributions and masses requires knowledge of the albedos that we do not yet possess. Under the assumption that the albedo does not vary systematically with size, the survey data indicate that the size distribution of the larger (diameters $\geq$50 km) KBOs are well described by a differential power law with an index near 4.0$\pm$0.5 (Trujillo et al., 2001). Models of agglomeration of KBOs in a cold disk are compatible with this index, suggesting that it might be a relic of the formation process. At small sizes, the role of collisional shattering should become important and the distribution is expected to flatten (slightly) towards the Dohnanyi value, an index of 3.5. Limited evidence from a deep Hubble Space Telescope (HST) survey suggests that this flattening has been detected (Bernstein et al., 2004): earlier and contradictory evidence from HST (Cochran et al., 1995) has apparently been invalidated.

Kuiper belt masses were initially estimated on the assumption that all KBOs have albedos of 0.04, like the nuclei of the Jupiter-family comets. These initial estimates gave masses $\sim$0.1 $M_\oplus$ (Jewitt et al., 1998). Recent measurements of large KBOs suggest albedos on average about three times larger but it is not known if this is generally true or if the high albedos apply only to the largest KBOs (we cannot yet measure the smaller ones directly). In any case, 0.1 $M_\oplus$ is an upper limit to the total mass. With mass scaling as $(\text{albedo})^{-3/2}$, the derived mass is $3^{3/2} \sim 5$ times smaller than first thought, corresponding to a few percent of an Earth mass. These estimates are still quite uncertain because we possess few reliable determinations of the albedos, because we do not know the densities of most KBOs and, especially, because we have meaningfully sampled only the inner regions of the Kuiper belt. For all these reasons, the relative masses of the various components of the Kuiper Belt are uncertain. A reasonably safe conclusion, however, is that the mass of the scattered disk objects is larger than the mass of the other components of the Kuiper belt (Trujillo et al., 2000).

4.4 Origin of the Structure

Understanding of the origin of dynamical structure in the Kuiper belt is at a juvenile stage and major changes can be expected as new survey data become available (soon,

from Pan-STARRS). There are several important parameters that must be fitted by the models. These include the (low) value of the total mass, its distribution amongst the various components (in the order scattered disk > classical belt > resonant population), the bounded distribution of semi-major axes of the classical objects (edge near the 2:1 resonance), the broad distributions of inclination and the bimodal distribution within the classical belt (and probably not elsewhere). While the number of observational constraints is already considerable, the number of degrees of freedom in models designed to fit the observations is much greater. Thus, the subject suffers from the classical problem of non-uniqueness. Interesting models are proposed and published, but many are based on initial conditions or other assumptions that are either arbitrary or untested. Still, it is interesting to speculate on the origin of the dynamical structure of the Kuiper belt.

The most plausible way to populate the resonances is through slow radial migration (Malhotra, 1995; Gomes, 2003b). A fraction of the KBOs encountered by a drifting resonance become captured and their inclinations and eccentricities may become enlarged as a result. Simple models suggest that migration of Neptune over $\sim$7 or 8 AU distances on time-scales near 10 Myr could account for the resonant populations. One puzzle is that the resonant populations are small ($\sim$10% of the total, possibly less) whereas migration models can be much more efficient. An explanation may lie in the jumpy nature of Neptune's migration, with the jumps being caused by individual interactions with massive bodies in the protoplanetary disk.

The cold component of the classical belt suggests that it is most closely related to (but still substantially thicker than) the original protoplanetary accretion disk. The existence of an edge at the 2:1 resonance may suggest that bodies in the cold population were dragged outwards by this resonance as Neptune migrated (Levison & Morbidelli, 2003). Otherwise we would have to suppose that the closeness of the edge and the resonance is merely a coincidence.

The scattered population shows signs of having been emplaced by long-term perihelic interactions with Neptune. While the implications of these belt components look secure, it is unclear how they fitted together in producing the Belt from a much thinner, more uniform and (probably) denser protoplanetary disk. One recent suggestion is particularly fascinating and, to avoid being drawn into a long description of the many models, we mention it here alone. Tsiganis et al. (2005) suppose that the early planetary system started with Jupiter and Saturn close to the 2:1 mean motion resonance (they are now close to, but not in, the 5:2 mean motion resonance with each other). Uranus and Neptune interacted gravitationally with each other and with Jupiter and Saturn. Torques between Neptune and a dense Kuiper belt caused a slow, outward migration of that planet. With the right assumptions of planetary orbit radius and Kuiper belt primordial density, the outward migration of Neptune can be adjusted to continue for hundreds of millions of years, eventually, pulling Jupiter and Saturn into the 2:1 resonance, whereupon strong interactions between these massive planets excite Neptune into a destructive interaction with the primordial belt, scattering its contents throughout the solar system. With the right choice of initial conditions, this model might account for the delayed late-heavy bombardment of the surface of the Moon (at about 3.8 - 3.9 Gyr) as a result of final destabilization of the trans-Neptunian region (Gomes et al., 2005). It would also produce the scattered disk from an initially confined

distribution of inclinations, and it might produce the hot component of the classical belt. The origin of the cold component is not well explained by this scenario.

4.5 Problem of the missing mass

The mass of the current Kuiper belt estimated from survey observations and limited numbers of albedo measurements lies in the 0.01 to 0.1 $M_\oplus$ range. Several indirect lines of evidence suggest that this is a small fraction of the initial mass and that, therefore, most of the initial mass has been lost. First, the surface density of the protoplanetary disk can be estimated from the distribution of the refractory materials in the giant planets. An extrapolation of this surface density across the region of the Kuiper belt predicts a mass ∼100 times larger than observed. Second, models in which the KBOs grow by binary accretion fail to produce KBOs of the sizes observed unless the protoplanetary disk density in the Kuiper belt is increased by factors of ∼100 or more (Kenyon & Luu, 1999). Thirdly, while the mechanism for the formation of binaries remains unclear, it is reasonably certain that binaries cannot form in the present-day low density environment. The binary formation models that have been suggested require formation in a much higher density Kuiper belt, perhaps 100 to 1000 times denser than now. Likewise, massive impacts capable of producing Pluto-Charon type binaries are now vanishingly rare. If they occurred at all, it must have been in an earlier, denser phase of the Kuiper belt.

If these indirect arguments are valid, how might the mass have been lost? The answer to this question is not known, but there are several conjectures in the literature. For example, some part of the initial mass might have been lost by dynamical erosion. Neptune cannot do the job, depleting the mass of the belt by only a factor of a few over the age of the solar system except for orbits in its immediate vicinity. A passing star might substantially erode the belt, but it is not obvious that the remnant left behind would be like the Kuiper belt in detail. Perhaps the mass was lost through collisional grinding. In this, the KBOs collide and shatter, producing a cascade of particles of sizes all the way down to dust. At the smallest sizes, these particles become responsive to radiation drag forces, and would spiral into the Sun. However, bodies larger than ∼50 km to 100 km are not easily shattered and the collisional grinding model only works if the initial size distribution in the Kuiper belt were so steep that most of the mass was held by the smallest (most destructable) bodies. It is unclear whether this size distribution ever prevailed.

Another possibility is that the lines of evidence for mass loss are misleading. The KBOs could have formed in a denser environment, perhaps at smaller heliocentric distances, perhaps aided by concentration of the condensible materials in the protoplanetary disk under the action of aerodynamic forces (Youdin & Chiang , 2004), followed by wholescale movement of this population out to the observed location. Understanding the reality and cause of the inferred mass loss is perhaps the biggest problem of the Kuiper belt.

5 Surface properties of KBOs

The study of the surface properties of KBOs is in its infancy: the field is probably at the same level of knowledge as for the main belt asteroids in the late 1970's. The main

reason is that the KBOs are extremely faint, even for telescopes in the 8-10m class. Also, secure orbits are needed to place the studied KBOs in the small fields of view of the instruments. This implies repeated observations of newly discovered objects, and recovery programs are generally not able to handle in real time the volume of discoveries. Of the thousand objects discovered, only half have well established orbits. Visible colors have been reported for ∼200, while only ∼50 objects have near infrared colors, and useful reflectance spectra are available for a mere handful.

Albedos and sizes are known only for a few objects (see Table 2 and Grundy et al., 2005). The visible flux measured from the object is proportional to the product of the geometric albedo and the square of the diameter. The thermally emitted flux, on the other hand, is proportional to (1 - albedo) times the diameter squared, because the fraction of the incident sunlight that is absorbed and thermally re-radiated is (1 - albedo). With surface temperatures near 40 K to 50 K, the Wien peak lies near 60μm to 75μm and is inaccessible from Earth. Observations of thermal emission have been made through sub-millimeter wavelength windows in the Earth's atmosphere but thermal observations nearer the emission peak require space-based data. NASA's spitzer satellite is taking such data now, but with a sensitivity less than originally planned for this mission, only a few dozen KBOs can be attempted. Observations in both the optical and thermal or sub-millimeter range are therefore required for one object to assess its albedo (and size).

5.1 Colors

The surface properties of KBO are assessed from the optical and near infrared light they reflect from the Sun, through broadband photometry and reflectance spectroscopy. Ideally, we would use spectra to study the surface compositions of the KBOs and related bodies. In practise, however, most KBOs are too faint for meaningful spectra to be acquired, and most investigators have resorted to broadband colors in the optical and near infrared wavelength regimes. Colors provide only very weak constraints on composition, but they are nevertheless useful in classifying the KBOs, in comparing them with other types of small solar system body, and in searching for correlations (e.g. with size, with orbital parameters) that might be physically revealing. Indeed, in the 1970's, surface color studies of main belt asteroids (orbiting between Mars and Jupiter) soon revealed a color pattern with heliocentric distance (McCord & Chapman, 1975; Zellner et al., 1977, 1985), unveiling a radial compositional structure of the primordial nebula at these distances (Gradie & Tedesco, 1982). It is therefore very tempting to try to reveal such patterns for the Kuiper belt population.

Quantitatively, the color is conveniently measured by the slope of the spectrum after division by the spectrum of the Sun, a quantity conventionally expressed as $S^{'}$ [%/1000Å] and known as the reflectivity gradient. This quantity can be derived from visible photometry. The least contested observational result is that the colors of the KBOs occupy a wide range, from neutral ($S^{'} \sim 0\%/1000$Å) to "very red" ($S^{'} \sim 60\%/1000$Å), indicating a wide diversity of surface types on KBOs (see Fig. 4). The question of the shape of the distribution of $S^{'}$ has received considerable attention. Most investigators report that $S^{'}$ is unimodally distributed while Tegler & Romanishin (1998, 2003) have reported a bimodal distribution, with KBOs being either nearly neutral, or very red and with very few in between. Later, Peixinho et al. (2003) reported that

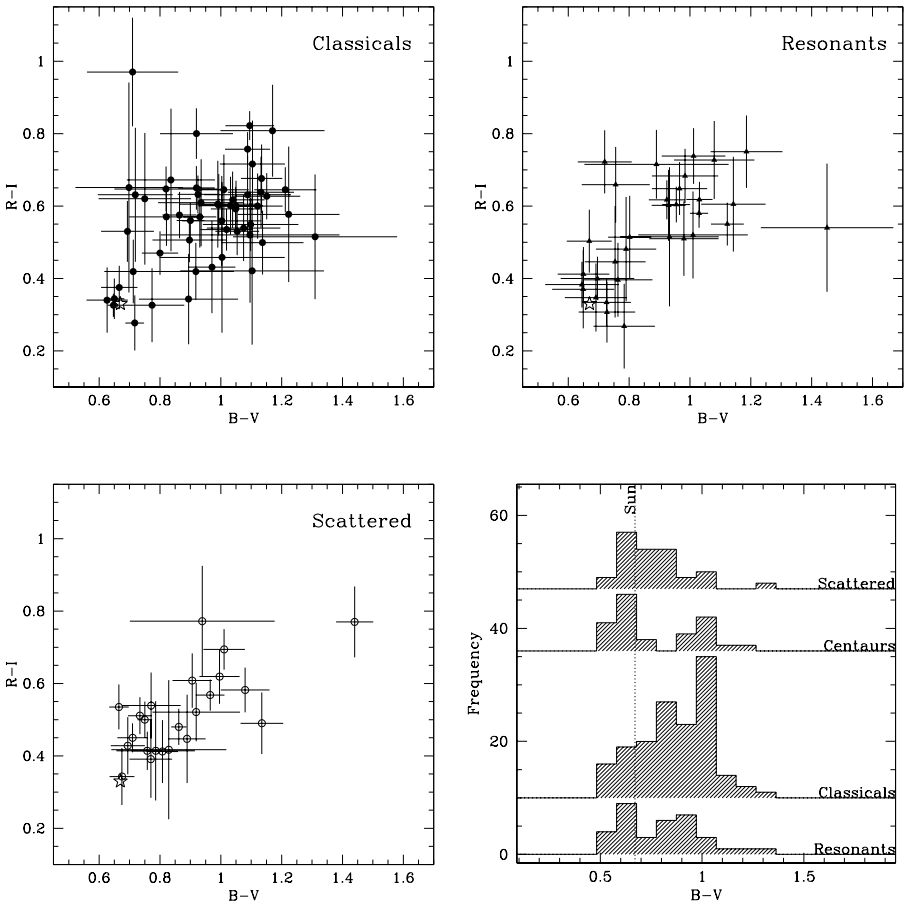

Fig. 4. COLORS OF KBOS (AS OF MARCH 2005) for the three dynamical subclasses: classical, resonant and scattered disk objects. Solar colors are represented by an open star. The bottom right plot represents a histogram of the B−V colors. Centaurs have been included for comparison.

Centaur colors are bimodally distributed while those of KBOs are not, and suggested that Tegler and Romanishin's finding of bimodal KBO colors was caused by their mixing of these two types of object into a single sample. The sum total of published data (as of 2005) show unimodal color distributions in the Kuiper belt but favor a bimodal distribution of Centaur surface colors (see Fig. 4 and 5). The unimodal vs. bimodal color question is important because it limits the range of options available for explaining the existence of the color diversity in the Kuiper belt.

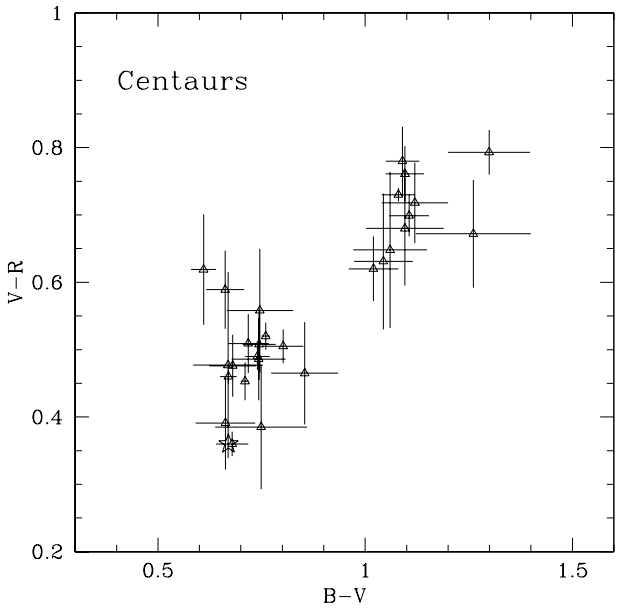

Fig. 5. COLORS OF CENTAURS: B-V vs V-R indexes (as of March 2005). The distribution appears bimodal for the 28 measured Centaurs. The star symbol represents the solar colors.

The origin of color diversity

Several explanations have been suggested for the origin of the amazing range of surface colors observed on KBOs. The simplest invokes a wide variety of chemical compositions. However, the temperature gradient across the Kuiper belt is about 30–50K, (assuming a blackbody in radiative equilibrium with the Sun), which is too low to produce a wide diversity in chemical compositions. Furthermore, there is no correlation of color with distance or semi-major axis, as might be expected if formation location and temperature were important. Gomes (2003a) describes how a population of highly inclined classical objects (the so-called "hot population") formed much closer to the Sun and was subsequently transported to the Kuiper belt by dynamical mechanisms. This could increase the range of formation temperatures of the KBOs and explain the hot/cold neutral/red color variations, but no specific relation between color and a potential formation location has been identified yet.

The second possibility is that the colors are evolutionary artifacts. Perhaps all KBOs had the same initial composition, a mix of solid organics, silicates and volatile ice, constrained by the cosmochemical abundances in the primordial nebula. Over time, external processing by irradiation from high energy particles (cosmic rays, solar wind and solar UV), by non disruptive collisions between KBOs and by the sublimation of volatiles could change the surface compositions.

The surface processes

Laboratory work shows that fresh (neutral colored) carbon-containing ices become gradually darker under irradiation by high energy particles, due to the progressive loss of hydrogen atoms and carbonization of the surface layers (Strazzulla & Johnson, 1991). Complete processing of a meter-thick crust of organic-rich material occurs on a time-scale of 10^{7-9} yrs (Shul'Man, 1972). In that context, the red colors of some of the KBOs are generally interpreted as the presence of an aged, irradiated organic-rich surface. However, while darkening is a general result, the effect of irradiation on color is less clear, being a complicated function of the material composition, particle fluency and even grain size distribution (Thompson et al., 1987; Moroz et al., 2004). Subject to this ambiguity, it is likely that high albedo neutral color surfaces refer to fresh icy material, while low albedo neutral surfaces should belong to highly irradiated objects. As a KBO surface ages, it should become darker and may change in color.

Non disruptive collisions between KBOs also may play a role as well in removing the dark red irradiation mantle at the location of the impact, revealing fresh neutrally colored underlying material. However, collision rates are not well constrained across the Kuiper belt, and big collisions that would result in an important rejuvenating of the KBO surfaces are statistically very unlikely.

Cometary activity is potentially efficient at creating uniform, neutral colored surfaces through sublimation (for example CO, and N_2 are both volatile at KBO temperatures) and the deposition of sub-orbital debris. Just as on comets, particles on the surface may be lifted by the outgassing and some fall back to create a uniform neutral surface. A burst of cometary-type activity might be triggered either by a collision impact, or by the increasing solar heat while orbiting near perihelion. Unfortunately, there is no observational evidence for routine cometary activity amongst KBOs and, except for occasional bursts triggered by local impacts, none is expected on most KBOs. The very largest objects may be an exception to this statement. We know that Pluto has a μbar atmosphere of N_2 and similarly large KBOs could likewise sustain sublimation-driven atmospheres and associated deposits of seasonally migrating frost.

Several numerical models implying the competition of two or three of these physical processes acting on KBOs surfaces over time succeeded in generally describing the color distribution observed (Jewitt & Luu, 2001; Delsanti et al., 2004). However, these models are incompatible with the Centaur color bimodality (see Figure 5) and with the color-inclination dependency of classical KBOs (see below).

The observed color trends

Apart from the wide spread of surface colors that prevail for the Kuiper belt as a whole (whether it is in the form of a continuous or bimodal distribution), more subtle trends were looked for. With the increasing number of color measurements, it became possible to look closer into the photometric properties of some of the dynamical subclasses. For classical KBOs, objects with perihelia inside about 40 AU show a wide range of optical colors while those beyond 40 AU tend to display only the reddest colors (Figure 6). This trend might be caused by an observational bias (the neutral colored objects with larger perihelion being for some reasons undetectable with the current observing tools), or simply these objects are absent. In both cases, a change of physical environment

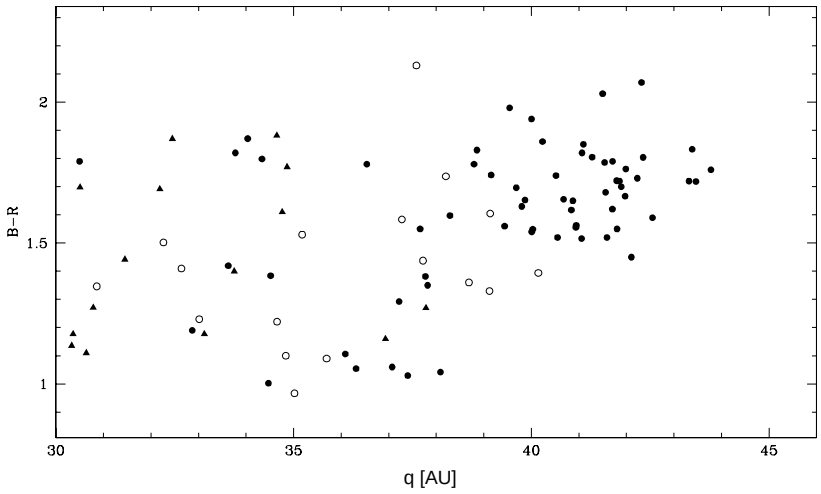

Fig. 6. $B-R$ color index plotted vs. perihelion distance, q [AU] for KBOs. At $q \leq 40$ AU, the KBOs show a wide scatter in $B-R$, from neutral to very red. For $q > 40$ AU, only red colors ($B-R \geq 1.5$), are found. The red, large q objects are also low inclinations members of the classical Kuiper belt population. Figure from Delsanti et al. (2004).

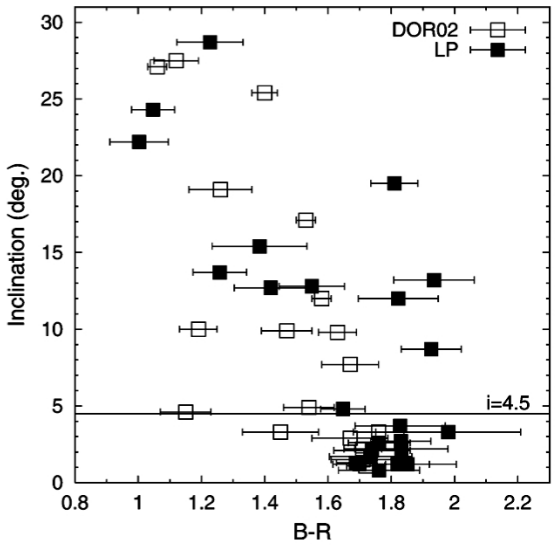

Fig. 7. $B-R$ color index plotted vs. orbital inclination i for two samples of classical KBOs from Peixinho et al. (2004). At $i \leq 4.5°$, the classical KBOs show only the reddest colors. For $i > 4.5°$, the whole color range from neutral to very red is displayed.

Table 5. KBOs and Centaurs with Water Ice Firmly Detected

Name	Type[a]	H[b]	Depth[c]	Reference[d]
(2060) Chiron	Cen	6.5	∼10%[e]	Foster et al. (1999), Luu et al. (2000)
(5145) Pholus	Cen	7.0	∼16%	Cruikshank et al. (1998)
(10199) Chariklo	Cen	6.4	20%	Brown & Koresko (1998)
(19308) 1996 TO_{66}	Cla	4.5	∼20%	Brown et al. (1999)
(31824) Elatus	Cen	10.1	24%?	Bauer et al. (2002)
(50000) Quaoar	Cla	2.6	∼22%	Jewitt and Luu (2004)
(83982) 2002 GO_9	Cen	9.1	∼16%	Doressoundiram et al. (2006)
(90482) Orcus	3:2	2.3	∼30%	de Bergh et al. (2005)

a: Dynamical type: 3:2 = resonant, Clas = Classical, Cen = Centaur
b: Absolute magnitude
c: 2 μm band depth as a fraction of the continuum
d: Prime reference: for brevity we list only one reference where several exist
e: The band depth is variable because of coma dilution. We list the maximum value.

at larger distances should be invoked. In the second case, this trend might support the idea of cometary activity amongst some KBOs, responsible for the blue objects at shorter perihelion distances, while for objects with larger perihelia, cometary activity is not expected. Collisional resurfacing model simulations by Thébault & Doressoundiram (2003) predicts this color-perihelion trend in the case of a disk truncated at 48 AU. The red, large perihelion classical KBOs also have the smallest inclinations (as displayed in Figure 7). The inclination cut-off ($\sim 4^o$) of the difference of color behavior (Fig. 7) is compatible with the concept of a primordial dynamically "cold" population (with small orbital inclinations) superimposed to a dynamically "hot" population (Levison & Stern, 2001) that formed elsewhere in the Solar System (Gomes, 2003a). However, there is currently no clear physical explanation why the cold population should display only the red colors, while the hot population should display the whole range of observed colors.
Other less significant trends scarcely show in the different photometry projects, but they are generally based on small number statistics and most of the time they fail to be found on other samples. As for the main asteroid belt, the most important and physically meaningful trends will strengthen with the increasing number of measured colors.

5.2 Spectra

The overtones and combination bands of common molecular bonds such as O-H, C-N, N-H occur in the near-infrared (1 to 2.5 μm) wavelength range, and the terrestrial atmosphere is also comparatively transparent there, at least from mountain sites where the atmospheric water column density is low. Information gleaned from spectra cannot in general be uniquely interpreted, because the reflection spectrum depends on many poorly-known factors in addition to the composition of the target material. For example, the physical state of the surface (whether it be solid, or particulate) plays a role in determining the scattering characteristics. In particulate surfaces, the grain size distribution, the porosity and even the grain shapes and temperature can be important.

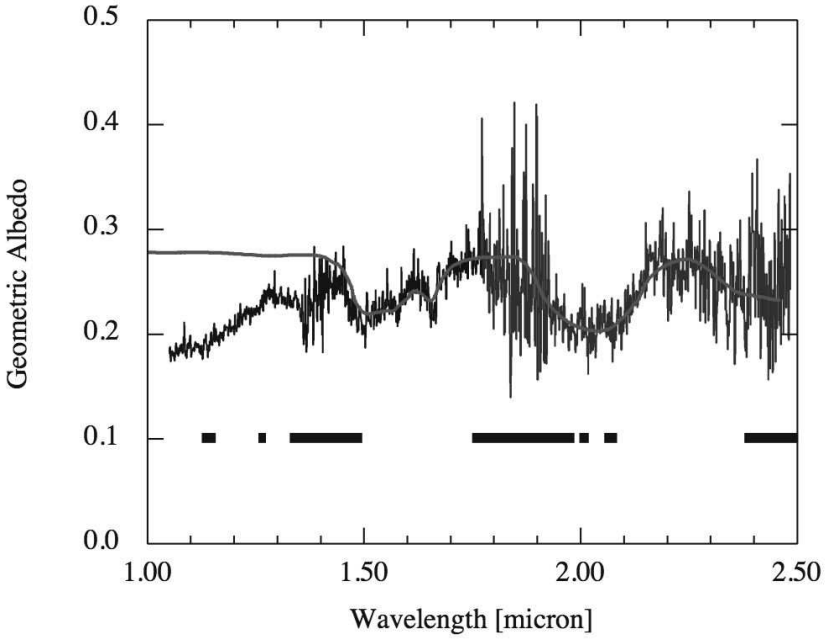

Fig. 8. Near infrared reflection spectrum of KBO (50000) Quaoar from the Subaru 8-m telescope. In addition to the broad bands due to water at 1.5 μm and 2.0 μm, a narrow feature at 1.65 μm proves that the surface ice is crystalline, not amorphous. Horizontal bars mark regions of strong absorption by the Earth's atmosphere. The solid line is a water ice spectrum overplotted on the data. From Jewitt and Luu (2004).

Nevertheless, near infrared absorptions are quite diagnostic of particular molecular bonds, providing a basis from which to make conjectures about molecular composition. The main practical problem is that the KBOs are faint and the resulting signal-to-noise ratios in KBO spectra are typically low. The discovery of the giant KBOs 2003 UB_{313} and 2005 FY_9, (see Sec. 2) lead to the detection of the first methane bands on a KBO besides Pluto. However, the most readily detected specie is water, which has been evidenced by its 2μm absorption in 3 KBOs and 5 Centaurs (see Table 5). As these lines are written, water was announced to be present at the surface of the giant KBO 2003 EL_{61}.

Observations of (50000) Quaoar show an absorption band at 1.65 μm that is found in crystalline (but not in amorphous) water ice (see Figure 8). The surface temperature of Quaoar is near $\sim$50 K or less, and at these low temperatures water should be stable indefinitely in its amorphous form. The presence of crystalline ice shows that the ice has been heated above the 100 to 110 K temperature at which amorphous ice transforms to the crystalline (cubic) form. The source of the heat needed to effect this transformation is unclear, but internal heating by the decay of radioactive elements followed by eruption onto the surface is possible. Impact heating could also transform

ice in the upper layers although how this happens without vaporizing the ice leading to its deposition as amorphous frost elsewhere on the frigid surface has not been demonstrated. A more serious question concerns the effect of high energy particles on the surface, from the cosmic rays and from particles in the solar wind. The effect of particle bombardment is to break the bonds in crystalline ice, leading to a transformation to the amorphous state. The timescale for the amorphization of ice is uncertain but short compared to the age of Quaoar: estimates range from 10^6 to 10^7 yrs. The fact that the ice is predominantly crystalline argues for comparatively recent emplacement, consistent with on-going endogenic activity.

Other species like ice of N2, NH_3, CO_2 etc, and other organic molecules are from cosmochemical arguments likely to be present at the surface of KBOs. To date, they fail to be detected; we suspect it is mainly for technological limitation reasons.

6 Related Objects

6.1 Centaurs

Centaurs are objects whose orbits bring them into close interaction with the giant planets: a practical (but not unique) definition is that the Centaurs have perihelia *and* semimajor axes between the orbits of Jupiter and Neptune. So defined, about 50 Centaurs are known, some like (2060) Chiron and 29P/Schwassmann-Wachmann 1 are cometary in nature, other like (5145) Pholus appear completely devoid of coma. These bodies have short dynamical lives owing to strong interactions with the giant planets. Characteristic lifetimes are 10^6 to 10^7 yrs, with a wide scatter (Tiscareno & Malhotra, 2003). Their source is most likely in the Kuiper belt: prevailing evidence suggests that the Centaurs are escaped members of the Scattered disk part of the Kuiper Belt population but other regions may also contribute to the Centaur populations. The main sinks of the Centaurs include ejection to the interstellar medium, capture by Jupiter followed by strong sublimation that leads these objects to be relabelled as comets of the Jupiter family, and collision with the planets or with the Sun. For these reasons, the Centaurs hold special interest in the study of the small body populations of the Solar system. They are closer, brighter counterparts to the KBOs, and they are precursors to the active nuclei of the Jupiter family comets.

In terms of their colors and surface compositions, the Centaurs appear similar to the KBOs: water ice is seen more commonly than other species. The great diversity of spectral types indicated by the wide range of colors of the KBOs is also present in the Centaur population in a bimodal version (see Figure 5). Characteristics from these two groups of surface colors are well represented by (2060) Chiron and (5145) Pholus. The former is spectrally neutral or slightly blue, and shows absorption at 2 μm due to water ice. No other features are detected in its spectrum. The latter is one of the reddest objects in the solar system (in the optical) and shows a structured near-infrared spectrum with bands due to water, a hydrocarbon possibly close to methanol, and olivine (Cruikshank et al., 1998). The very red optical spectrum is commonly attributed to an organic surface (most likely containing N_2 and CH_4) although, lacking discrete optical features, no unique diagnosis of the organic matter has been made.

6.2 Comets

Comets were initially envisioned as the most pristine material in the Solar System, as expected from relics from the accretion disk of the Sun. The nuclei of long period comets (that most likely formed in the Oort cloud and remained there for a long period of time) are still considered as true fossils. However, it is now believed that the nuclei of short period comets (the "Jupiter Family") have originated in the Kuiper belt, in the form of collisional fragments. In that case, short period comet nuclei have been somewhat processed, either by the heat of their parent body (if the latter is large enough to sustain heat from radiogenic decay), or by the physical processes that occured during the collision that generated them. To test this scenario, surface colors of short period comets are compared to those of KBOs (Hainaut & Delsanti, 2002; Jewitt, 2002; Doressoundiram et al., 2005). Colors of short period comets are not compatible with the observed colors of KBOs and Centaurs. The "ultrared matter" that is a unique characteristic of KBOs is rare or absent on the surface of short period comets nuclei. The most likely explanation is short period comets nuclei underwent different resurfacing processes during their journey from the Kuiper belt to their present location. For example, cometary activity is a short timescale process that resurfaces the nuclei with neutral colored suborbital particles that were lifted by the sublimation of the volatiles inside the orbit of Jupiter. This process might also be responsible for the lack of intermediate colors amongst the Centaurs. As a conclusion, short period comets, due to their most probable origin in the Kuiper belt and the subsequent thermal and physical processing they underwent, might not be the fossils the planetary scientists long dreamed of.

6.3 Irregular Satellites

The irregular satellites of the giant planets have large, eccentric and highly inclined orbits. Most known examples are retrograde, in fact, and the only plausible explanation is that they were captured by their respective planets probably long before the present epoch and perhaps in association with planet formation. The source region from which the irregular satellites were captured is not known. One possibility is that the irregular satellites are planetesimals that were initially in similar orbits but which narrowly escaped incorporation into the growing giant planets. In this case, it would be appropriate to think of the irregulars as samples of the material that agglomerated to form the massive, dense cores of the giant planets. Another possibility, currently growing in fashion, is that the irregulars were captured from distant locations in the Kuiper Belt. In this case, the irregulars could be considered as (more) local samples of material from the outer reaches of the Solar system.

Saturn's largest irregular satellite, Phoebe, has been studied close-up by NASA's Cassini spacecraft (Figure 9). The surface is heavily cratered but, otherwise, not remarkable compared to the surfaces of other small bodies that have been imaged at similar resolution. The density of Phoebe measured from gravitational deflections of the Cassini spacecraft (Porco et al., 2005) is 1630 ± 45 kg m^{-3}, consistent with a rock/ice mixture as the bulk composition. Johnson & Lunine (2005) assert that this high density points to a Kuiper belt origin, but the connection between density and formation location is unclear. Clark et al. (2005) and Esposito et al. (2005) detected numerous ices and other compounds on Phoebe that they believe point to a Kuiper belt source. However, the possibility that the surface is coated by ices delivered by cometary impact

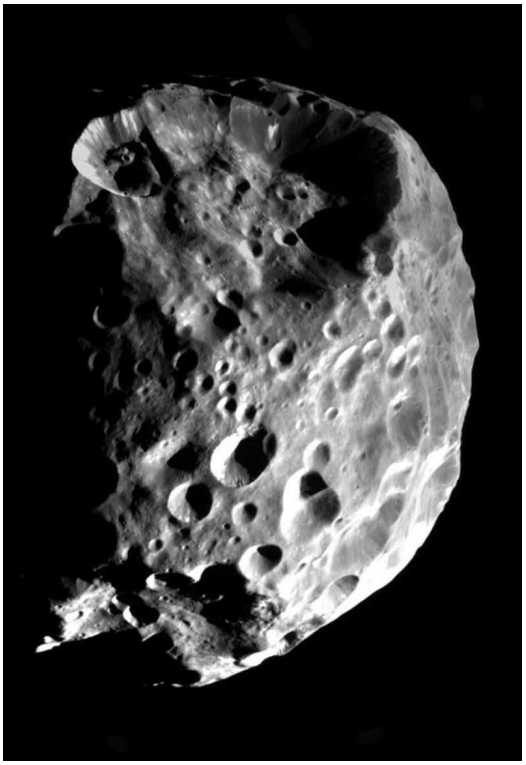

Fig. 9. Saturn satellite Phoebe imaged by the NASA Cassini spacecraft. Image courtesy Cassini Imaging Team and NASA/JPL/SSI.

cannot be discounted. Therefore, while we possess data of staggering resolution and quality on Phoebe, its origin is unclear.

The capture mechanism for irregular satellites is unknown. The favored hypothesis - gas drag in the bloated atmospheres of the young giant planets - might apply at Jupiter and Saturn where the total gas mass is large (the gas giants are >90% hydrogen and helium by mass). Uranus and Neptune also possess irregulars, however, and these ice giant planets are comparatively gas free, and formed by a process different from that which formed the gas giants. Three -body interactions (two small bodies in an encounter within the Hill sphere of the larger planet) might be capable of producing capture around both gas and ice giants, but the details of this mechanism have not been fully worked out. An intriguing new observation is that, measured down to a given limiting size, the four giant planets all possess about the same number of irregular satellites. To within a factor of ∼2 they all have ∼100 irregulars larger than 1 km in radius (Jewitt & Sheppard, 2005). This strange result, which is not predicted by any of the suggested satellite capture models, surely tells us something of importance about the origin of the irregulars, whether in the Kuiper belt or not.

Acknowledgments

This work was supported by a grant to DJ from the NASA Planetary Astronomy Program and by the NASA Astrobiology Institute under Cooperative Agreement No. NNA04CC08A issued through the Office of Space Science

References

Allen, R. L., Bernstein, G. M., & Malhotra, R. 2001, The Edge of the Solar System. ApJ Letters, 549, L241

Bauer, J. M., Meech, K. J., Fernández, Y. R., Farnham, T. L., & Roush, T. L. 2002, Observations of the Centaur 1999 UG5: Evidence of a Unique Outer Solar System Surface. PASP, 114, 1309

de Bergh, C., Delsanti, A., Tozzi, G. P., Dotto, E., Doressoundiram, A., & Barucci, M. A. 2005, The surface of the transneptunian object 90482 Orcus. A&A, 437, 1115

Bernstein, G. M., Trilling, D. E., Allen, R. L., Brown, M. E., Holman, M., & Malhotra, R. 2004, The Size Distribution of Trans-Neptunian Bodies. AJ, 128, 1364

Brown, R. H., Cruikshank, D. P., & Pendleton, Y. 1999, Water Ice on Kuiper Belt Object 1996 TO_{66}. ApJ Letters, 519, L101

Brown, M. E., Trujillo, C., & Rabinowitz, D. 2004, Discovery of a Candidate Inner Oort Cloud Planetoid. ApJ, 617, 645

Brown, M.E., Trujillo, C.A., Rabinowitz, D.L. 2005, Discovery of a planetary-sized object in the scattered Kuiper belt, submitted to ApJ Letters

Brown, M.E, van Dam, M.A, Bouchez, A.H., Le Mignant D., Campbell, R.D., Chin, A., Conrad, A. et al. 2005, Satellites of the largest Kuiper belt objects, submitted to ApJ Letters

Brown, M.E, Bouchez, A.H., Rabinowitz, D., Sari, R., Trujillo, C.A., van Dam, M.A, Campbell, R.D. et al 2005, Keck Observatory Laser Guide Star Adaptive Optics Discovery and Characterization of a Satellite to the Large Kuiper Belt Object 2003 EL61. ApJ Letters, 632, L45

Brown, M. E., & Koresko, C. C. 1998, Detection of Water Ice on the Centaur 1997 CU 26. ApJ Letters, 505, L65

Canup, R. M. 2005, A Giant Impact Origin of Pluto-Charon. Science, 307, 546

Clark, R. N., et al. 2005, Compositional maps of Saturn's moon Phoebe from imaging spectroscopy. Nature, 435, 66

Cochran, A. L., Levison, H. F., Stern, S. A., & Duncan, M. J. 1995, The Discovery of Halley-sized Kuiper Belt Objects Using the Hubble Space Telescope. ApJ, 455, 342

Cruikshank, D. P., et al. 1998, The Composition of Centaur 5145 Pholus. Icarus, 135, 389

Delsanti, A., Hainaut, O., Jourdeuil, E., Meech, K. J., Boehnhardt, H., & Barrera, L. 2004, Simultaneous visible-near IR photometric study of Kuiper Belt Object surfaces with the ESO/Very Large Telescopes. A&A, 417, 1145

Doressoundiram, A., Peixinho, N., Doucet, C., Mousis, O., Barucci, M. A., Petit, J. M., & Veillet, C. 2005, The Meudon Multicolor Survey (2MS) of Centaurs and trans-neptunian objects: extended dataset and status on the correlations reported. Icarus, 174, 90

Doressoundiram, A., Barucci, M.A., Tozzi, G.P., Poulet, F., Boehnhardt, H., de Bergh, C. and Peixinho, N. 2006, Spectral characteristics and modeling of the trans-neptunian object (55565) 2002 AW197 and the Centaurs (55576) 2002 GB10 and (83982) 2002 GO9. PSS in press

Elliot, J. L., Dunham, E. W., Bosh, A. S., Slivan, S. M., Young, L. A., Wasserman, L. H., & Millis, R. L. 1989, Pluto's atmosphere. Icarus, 77, 148

Elliot, J. L., Ates, A., Babcock, B. A., Bosh, A. S., Buie, M. W., Clancy, K. B., Dunham, E. W., et al. 2003, The recent expansion of Pluto's atmospher, Nature, 424, 165

Elliot, J. L., et al. 2005, The Deep Ecliptic Survey: A Search for Kuiper Belt Objects and Centaurs. II. Dynamical Classification, the Kuiper Belt Plane, and the Core Population. AJ, 129, 1117

Emel'yanenko, V. V., Asher, D. J., & Bailey, M. E. 2003, A new class of trans-Neptunian objects in high-eccentricity orbits. MNRAS, 338, 443

Esposito, L. W., et al. 2005, Ultraviolet Imaging Spectroscopy Shows an Active Saturnian System. Science, 307, 1251

Foster, M. J., Green, S. F., McBride, N., & Davies, J. K. 1999, NOTE: Detection of Water Ice on 2060 Chiron. Icarus, 141, 408

Gladman, B., Holman, M., Grav, T., Kavelaars, J., Nicholson, P., Aksnes, K., & Petit, J.-M. 2002, Evidence for an Extended Scattered Disk. Icarus, 157, 269

Goldreich, P., Lithwick, Y., & Sari, R. 2002, Formation of Kuiper-belt binaries by dynamical friction and three-body encounters. Nature, 420, 643

Gomes, R. 2003, Planetary science: Conveyed to the Kuiper belt. Nature, 426, 393

Gomes, R. S. 2003, The origin of the Kuiper Belt high-inclination population. Icarus, 161, 404

Gomes, R., Levison, H. F., Tsiganis, K., & Morbidelli, A. 2005, Origin of the cataclysmic Late Heavy Bombardment period of the terrestrial planets. Nature, 435, 466

Gradie, J., & Tedesco, E. 1982, Compositional structure of the asteroid belt. Science, 216, 1405

Grundy, W. M., & Fink, U. 1996, Synoptic CCD Spectrophotometry of Pluto Over the Past 15 Years. Icarus, 124, 329

Grundy, W. M., Noll, K. S., & Stephens, D. C. 2005, Diverse albedos of small trans-neptunian objects. Icarus, 176, 184

Hainaut, O. R., & Delsanti, A. C. 2002, Colors of Minor Bodies in the Outer Solar System. A statistical analysis. A&A, 389, 641

Holman, M. J., & Wisdom, J. 1993, Dynamical stability in the outer solar system and the delivery of short period comets. AJ, 105, 1987

Ida, S., Larwood, J., & Burkert, A. 2000, Evidence for Early Stellar Encounters in the Orbital Distribution of Edgeworth-Kuiper Belt Objects. ApJ, 528, 351

Jewitt, D., & Luu, J. 1993, Discovery of the candidate Kuiper belt object 1992 QB1. Nature, 362, 730

Jewitt, D., Luu, J., & Trujillo, C. 1998, Large Kuiper Belt Objects: The Mauna Kea 8K CCD Survey. AJ, 115, 2125

Jewitt, D. C. 2002, From Kuiper Belt Object to Cometary Nucleus: The Missing Ultrared Matter. AJ, 123, 1039

Jewitt, D. C., & Luu, J. X. 2001, Colors and Spectra of Kuiper Belt Objects. AJ, 122, 2099

Jewitt, D. C., and Luu, J. 2004, Crystalline water ice on the Kuiper belt object (50000) Quaoar. Nature, 432, 731

Jewitt, D., & Sheppard, S. 2005, Irregular Satellites in the Context of Planet Formation. Space Science Reviews, 116, 441

Johnson, T. V., & Lunine, J. I. 2005, aturn's moon Phoebe as a captured body from the outer Solar System. Nature, 435, 69

Kenyon, S. J., & Luu, J. X. 1999, ApJ, Accretion in the Early Outer Solar System. 526, 465

Levison, H. F., & Morbidelli, A. 2003, The formation of the Kuiper belt by the outward transport of bodies during Neptune's migration. Nature, 426, 419

Levison, H. F., & Stern, S. A. 2001, On the Size Dependence of the Inclination Distribution of the Main Kuiper Belt. AJ, 121, 1730

Licandro, J. Pinilla-Alonso, N., Pedani, M., Oliva. E., Tozzi, G.P. and Grundy, W. 2006, The methane ice rich surface of large TNO 2005 FY9: a Pluto-twin in the trans-neptunian belt?, A&A Letters, in Press

Luu, J. X., Jewitt, D. C., & Trujillo, C. 2000, Water Ice in 2060 Chiron and Its Implications for Centaurs and Kuiper Belt Objects. ApJ Letters, 531, L151

Malhotra, R. 1995, The Origin of Pluto's Orbit: Implications for the Solar System Beyond Neptune. AJ, 110, 420

McCord, T. B., & Chapman, C. R. 1975, Asteroids - Spectral reflectance and color characteristics. ApJ, 195, 553

Morbidelli, A., & Levison, H. F. 2004, Scenarios for the Origin of the Orbits of the Trans-Neptunian Objects 2000 CR105 and 2003 VB12 (Sedna) AJ, 128, 2564

Morbidelli, A., Emel'yanenko, V. V., & Levison, H. F. 2004, Origin and orbital distribution of the trans-Neptunian scattered disc. MNRAS, 355, 935

Moroz, L., Baratta, G., Strazzulla, G., Starukhina, L., Dotto, E., Barucci, M. A., Arnold, G., & Distefano, E. 2004, Optical alteration of complex organics induced by ion irradiation: 1. Laboratory experiments suggest unusual space weathering trend. Icarus, 170, 214

Peixinho, N., Doressoundiram, A., Delsanti, A., Boehnhardt, H., Barucci, M. A., & Belskaya, I. 2003, Reopening the TNOs color controversy: Centaurs bimodality and TNOs unimodality. A&A, 410, L29

Peixinho, N., Boehnhardt, H., Belskaya, I., Doressoundiram, A., Barucci, M. A., & Delsanti, A. 2004, ESO large program on Centaurs and TNOs: visible colors-final results. Icarus, 170, 153

Porco, C. C., et al. 2005, Cassini Imaging Science: Initial Results on Phoebe and Iapetus. Science, 307, 1237

Rabinowitz, D.L, Barkume, K., Brown, M.E., Roe, H., Schwartz, M., Tourtellotte, S., Trujillo, C. 2005, Photometric observations constraining the size, shape and albedo of 2003 EL61, a rapidly rotating, Pluto-sized object in the Kuiper Belt, submitted to ApJ

Sheppard, S. S., & Jewitt, D. 2004, Extreme Kuiper Belt Object 2001 QG298 and the Fraction of Contact Binaries. AJ, 127, 3023

Shul'Man, L. M. 1972, The Chemical Composition of Cometary Nuclei, IAU Symp. 45: The Motion, Evolution of Orbits, and Origin of Comets, 45, 265

Sicardy, B., et al. 2003, Large changes in Pluto's atmosphere as revealed by recent stellar occultations. Nature, 424, 168

Strazzulla, G., & Johnson, R. E. 1991, ASSL Vol. 167: IAU Colloq. 116: Comets in the post-Halley era, 243

Tegler, S. C., & Romanishin, W. 1998, Two distinct populations of Kuiper-belt objects. Nature, 392, 49

Tegler, S. C., & Romanishin, W. 2003, Resolution of the kuiper belt object color controversy: two distinct color populations. Icarus, 161, 181

Thébault, P., & Doressoundiram, A. 2003, Colors and collision rates within the Kuiper belt: problems with the collisional resurfacing scenario. Icarus, 162, 27

Thompson, W. R., Murray, B. G. J. P. T., Khare, B. N., & Sagan, C. 1987, Coloration and darkening of methane clathrate and other ices by charged particle irradiation - Applications to the outer solar system. JGR, 92, 14933

Tiscareno, M. S., & Malhotra, R. 2003, The Dynamics of Known Centaurs. AJ, 126, 3122

Tombaugh, C. W. 1961, The Trans-Neptunian Planet Search. Planets and Satellites, edited by Gerard P. Kuiper and Barbara M. Middlehurst Chicago: University of Chicago Press, 1961, p.12

Trujillo, C. A., Jewitt, D. C., & Luu, J. X. 2000, Population of the Scattered Kuiper Belt. ApJ Letters, 529, L103

Trujillo, C. A., Jewitt, D. C., & Luu, J. X. 2001, Properties of the Trans-Neptunian Belt. AJ, 122, 457

Trujillo, C. A., & Brown, M. E. 2002, A Correlation between Inclination and Color in the Classical Kuiper Belt ApJ Letters, 566, L125

Trujillo, C. A., & Brown, M. E. 2003, The Caltech Wide Area Sky Survey, Earth Moon and Planets, 92, 99

Tsiganis, K., Gomes, R., Morbidelli, A., & Levison, H. F. 2005, Origin of the orbital architecture of the giant planets of the Solar System. Nature, 435, 459

Veillet, C., et al. 2002, The binary Kuiper-belt object 1998 WW31. Nature, 416, 711

Weaver, H. A., et al. 2005, S/2005 P 1 and S/2005 P 2. IAU circular, 8625, 1

Weidenschilling, S. J. 2002, On the Origin of Binary Transneptunian Objects. Icarus, 160, 212

Youdin, A. N., & Chiang, E. I. 2004, ApJ, Particle Pileups and Planetesimal Formation. 601, 1109

Zellner, B., Andersson, L., & Gradie, J. 1977, UBV photometry of small and distant asteroids. Icarus, 31, 447

Zellner, B., Tholen, D. J., & Tedesco, E. F. 1985, The eight-color asteroid survey - Results for 589 minor planets. Icarus, 61, 355